Contract No:

This document was prepared in conjunction with work accomplished under Contract No. DE-AC09-08SR22470 with the U.S. Department of Energy (DOE) Office of Environmental Management (EM).

Disclaimer:

WSRC-TR-2003-00150

Evaluation of Borated Aluminum Products for Criticality Control in 235-F

Savannah River Technology Center
Strategic Materials Technology Department
Materials Technology Section

Publication Date: April 2003

Westinghouse Savannah River Company
Savannah River Site
Aiken, SC 29808

This document was prepared in connection with work done under Contract No. DE-AC09-96SR18500 with the U. S. Department of Energy

This page left intentionally blank

TABLE OF CONTENTS

LIST OF FIGURES

LIST OF TABLES

1. Executive Summary

Plutonium-containing materials are destined for storage in the 235-F vault. The projected amount of stored materials will require the presence of neutron absorber materials. The leading design concept is for the neutron absorber materials to be in non-load-bearing borated aluminum plates lining the walls of the vault. A comprehensive evaluation of the borated aluminum plate materials was performed to identify a suitable material, and verify that these materials would remain effective as neutron absorbers under normal service conditions and for design-basis events, including the fire accident scenario, throughout a 20-year service life.

Aluminum 1100 with boron additions is the recommended neutron absorber material for plutonium material storage in the 235-F vault based on boron loading capacity and durability in the storage environment. Borated aluminum 1100 is commercially available up to 4.5 wt. % boron. A detailed comparison was made of the physical, mechanical, and corrosion properties of borated aluminum alloy 1100 to standard alloy 1100-O[1] to demonstrate near-equivalency in properties and to justify application of alloy 1100-O properties to the borated product as needed for the degradation analysis.

The expected degradation of the borated aluminum is extremely low for storage conditions, including the bounding scenario of an aggressive atmospheric condition. A maximum loss of 0.00029 inches/year would be expected under potentially aggressive atmospheric conditions and would result in a fractional loss of only 0.42 wt. % of the boron present in a 7mm plate for a 20-year storage period. The fraction of Boron-10 consumption by spontaneous neutrons is expected to be less than 10^{-8} for the 20-year storage in 235-F fully loaded with Pu materials.

The borated aluminum alloy 1100 will be thermally stable and unaltered up to near-melt temperature (643°C). Mechanical testing data at elevated temperatures show that the strengths (yield and ultimate) of the borated aluminum alloy 1100 are equal or greater than those of aluminum alloy 1100-O, but with less ductility. A fire accident scenario would not adversely impact the configuration or the neutron-absorbing performance of non-load-bearing plates.

No additional surveillances are needed to verify these conclusions. However, if a design-basis fire or other off-normal event occurs during the storage period, it is recommended to verify that the conditions of the event have been covered by those assumed in this report.

2. Introduction

2.1 Scope of Project

As part of an initiative to store plutonium-containing materials in F area, a vault is being constructed in 235-F. This vault will house plutonium and plutonium-containing materials in DOE approved 3013 canisters around the perimeter walls in specially designed racks and behind shielding to reduce criticality concerns and minimize dose to personnel. Figure 2.1 shows a photograph of a rack constructed for this facility. The rack is designed for the 3013 canisters to slip into each slot and be held at a fixed angle. Figure 2.2 shows the schematic of the vault, which illustrates the layout of these racks. The capacity of the vault is almost 2000 canisters and the layout must be designed to ensure criticality safety.

An initial criticality safety analysis was performed based on the proposed layout and given rack design. A K_{safe} of 0.95 is the criterion for criticality safety in this vault and must be maintained for any storage configuration. The initial calculations (w/out the addition of engineered neutron absorbers) showed that

[1] -0 designates the fully annealed condition

K_{eff} surpassed the K_{safe} for several cases. Figure 2.3 illustrates this point, showing the K_{eff} for two cases above 0.95. Further analysis determined that a K_{eff} could be maintained below 0.95 if additional neutron absorbers were incorporated into the vault design. After surveying several materials, a borated aluminum product was selected as a potential candidate for criticality control in the vault.

Figure 2.4 is a representation of effect of two alloys on the K_{eff} for the storage configuration. Aluminum alloy 1100 is a non-heat treatable aluminum alloy that is used when corrosion resistance and ductility (i.e., elongation to failure) are more desirable than strength. Alloy 1100 with boron added is available as rolled plate or sheet (desirable for shielding), or in a variety of wrought shapes up to 4.5 wt. % boron. Alloy 6351 is a heat-treatable alloy used in extrusions and is preferred when moderate strength, coupled with good corrosion resistance, is needed for a given application. The availability of this alloy with boron additions is usually limited to extruded parts (i.e. bar, rods and strip) containing up to 2 wt. % boron. The intended design was to hang sheets of the borated material on the wall behind each rack. As is evident from Figure 2.4, almost any thickness or loading of boron in these alloys is sufficient to maintain the K_{eff} below K_{safe} (i.e., 0.95). Considering the rudimentary nature of the intended design and enhanced boron loading available in the 1100 alloy the decision was made to evaluate this alloy for use in the 235-F storage vault.

Figure 2.1: Photograph of a potential rack for 235-F [1]

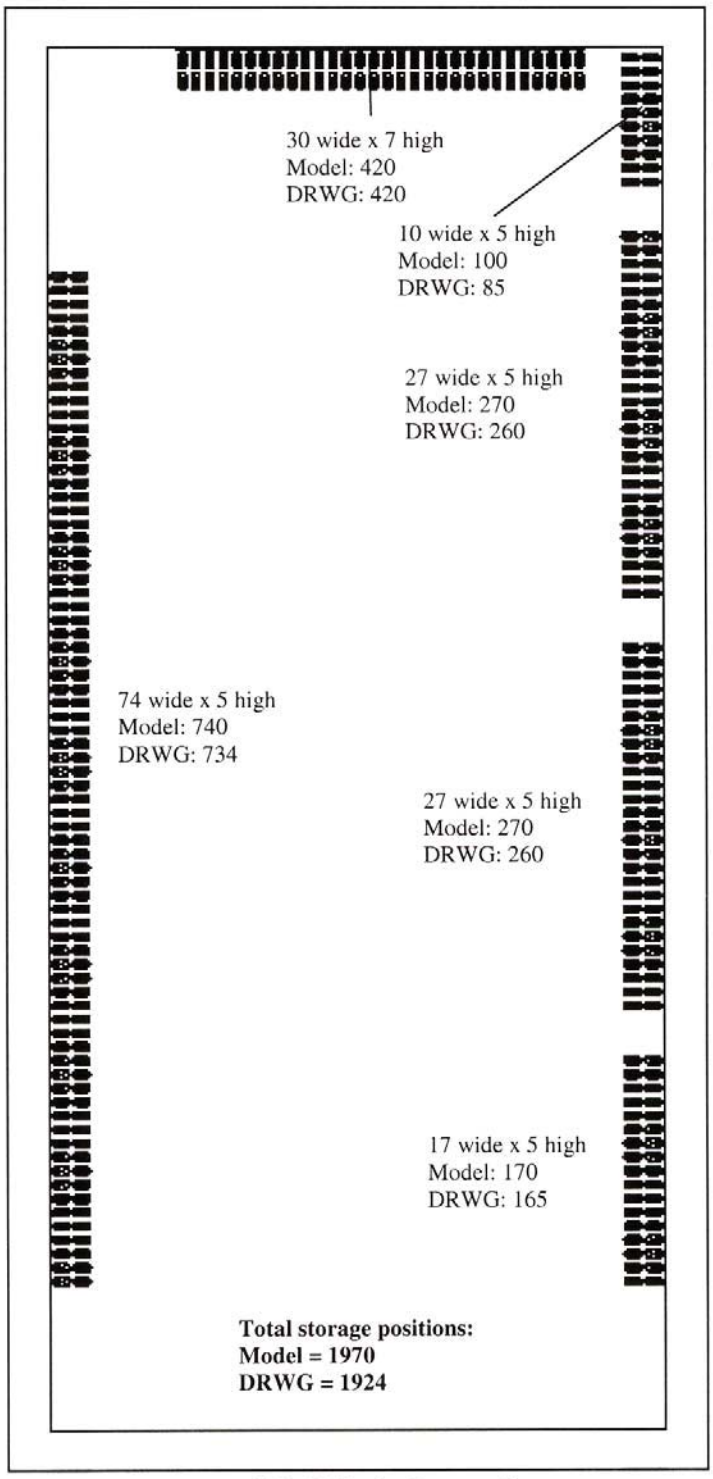

Figure 2.2: Proposed Layout for 235-F Vault [1]

Figure 2.3: Preliminary criticality analysis for proposed storage configuration [1]

4.4 kg Pu metal as a cylinder with H/D = 1 inside 3013 containers (96% Pu-239 & 4% Pu-240)

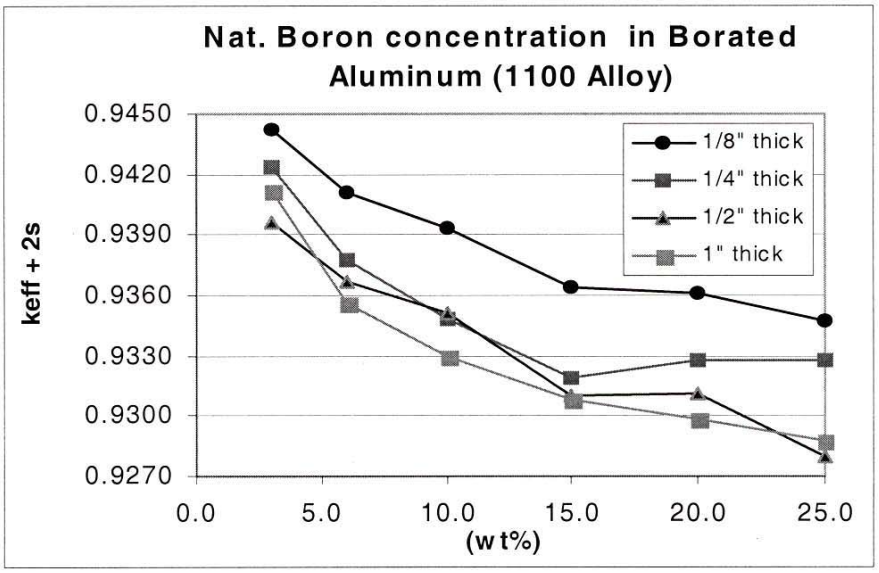

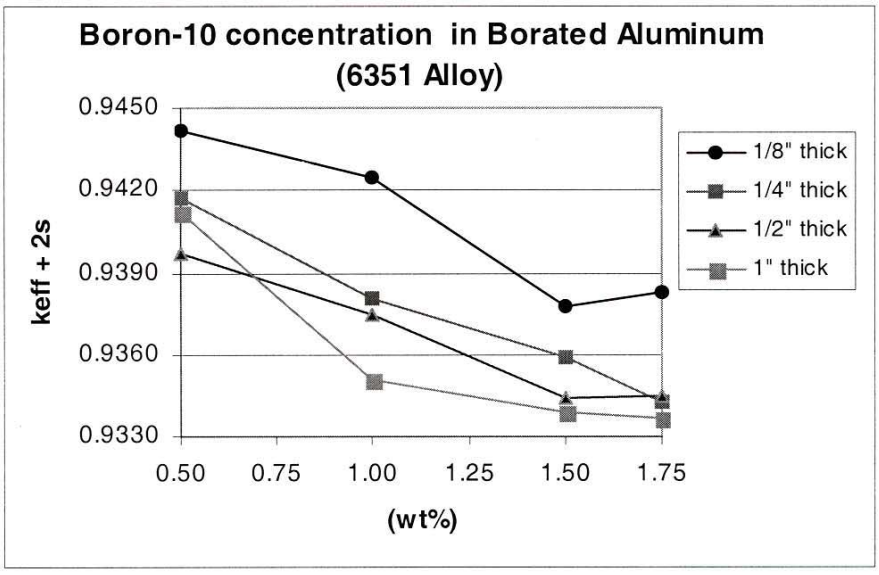

Figure 2.4: Effect of boron content and thickness in borated aluminum alloys on K_{eff} of proposed storage configuration [1]. (natural boron concentration = 5.47 * B-10 concentration)

2.2 Normal and Off-Normal Service Environments

Normal service environments concern the environment that the neutron absorbing system would be exposed to during its intended service life. Off-normal service environments are those environments that result from off-normal events, such as fire or accident scenarios.

Aluminum alloys containing boron would be used in service in a plutonium storage facility in F-area. The service environments that exist in the plutonium storage facility for 235-F are consistent with other indoor operations on site. No water will be allowed in this area other than that present in the air. The design rack is made of stainless steel and will be mounted close to concrete walls. Typical summer conditions would be 60%RH and 27ºC (80 ºF). Typical winter conditions would be 35%RH and 21ºC (70 ºF). Although these environments are controlled by heating and ventilation systems, occasional outages and process upsets could result in temperatures as low as –1 ºC (30 ºF) in the winter for a few hours duration and temperatures in the summer as high as 99 ºC (211 ºF) [2]. The design life of the facility is 20 years.

The environment should be considered an indoor environment (with of w/out air conditioning). The levels of airborne pollutants experienced in the facility well below levels of pollutants observed in urban, industrial or coastal environments. Industrial pollutants most commonly present in air are gases, suspended liquids and solids that contain a wide variety of chemical compounds. The most common deleterious substances from a corrosion standpoint contain sulfur, nitrogen and chlorine. Many of these substances, when combined with water form SO_4^{2-}, NO_2^- and Cl^- ions which have been shown to be detrimental in atmospheric corrosion. There are no processes in the building that would generate any form of SO_4^{2-}, NO_2^- and Cl^-, so only what would normally be in building air would be experienced. Figure 2.5 are area maps [3] illustrating the variations of these species for of the southeastern region of U. S. Green depicts a relatively low concentration of chemical species and red depicts a relatively high concentration. Field pH is a measure of the acidity of rainfall and is usually lowest in industrial regions. Nitrate and Sulfate are industrial pollutants and are observed in relatively high quantities in the industrial environments. Chloride content increases with proximity to the coastal shores. The region where the Savannah River Site is located shows low to moderate levels of all of these compounds. The South Carolina Bureau of Air Quality shows levels in and around Aiken County as low [4, 5]. Table 2.1 lists the average values for measured species in and around Aiken County.

The proposed methods of installation for neutron absorbers involve one of two scenarios. The first scenario uses organic cement to glue the aluminum against the concrete wall and installing a galvanized steel grating over top the borated aluminum. The second scenario attaches the aluminum to the concrete wall with anchor bolts place on 2 foot or 4 foot centers along the top and bottom edge of the panel.

The design basis fire event is currently under evaluation. Temperature profiles and duration of each incident depends several factors. However, because of adequate ventilation and limited combustible material in the area, it is common for fire analyses in facilities of this nature to yield average room temperatures below 120 ºC and less than one hour. [6].

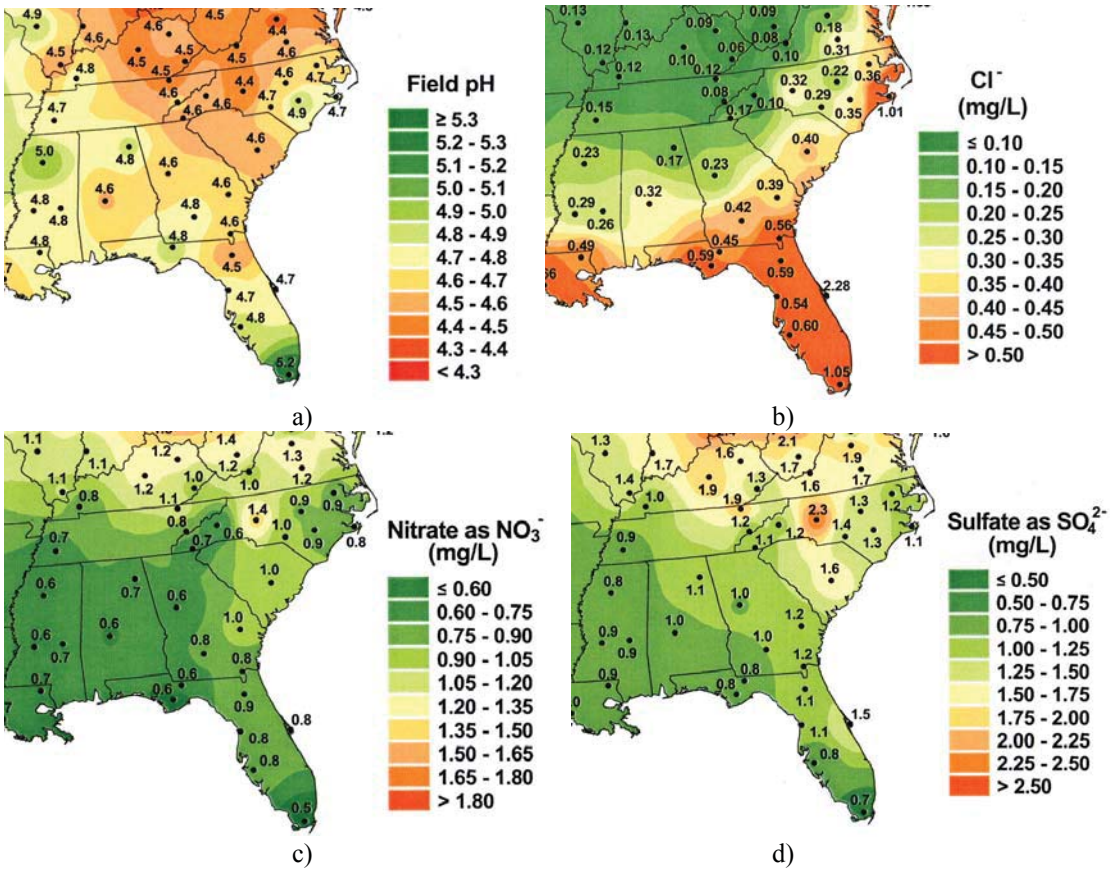

Figure 2.5: Atmospheric precipitation weighted averages for the southeastern region of the U.S. in 2001 (a) field measurements of pH, b) chloride, c) nitrate and d) sulfate ions) [3].

Table 2.1: Annual Measured Average Levels of Polutants in and around Aiken County [4,5]

Pollutant	Year 1999	Year 2001
Total Suspended Particles (TSP)	38 μg/m^3	32 μg/m^3
SO_2	0.003 ppm	0.002 ppm
NO_2	0.005 ppm	0.015 ppm
O_3	0.125 ppm *	0.113 ppm *
pH of Rain	4.4	4.5

* levels are 1h daily maximum values

2.3 Proposed Evaluation

A materials compatibility evaluation was necessary for the borated aluminum product(s) as a part of the 235-F storage vault design project. SRTC was asked to perform the evaluation on the functionality and boron efficacy of the intended design. This would ensure that the design team could correctly implement the material in a fashion that provided adequate stability for the service life of the vault (20 years).

In order to conduct a complete evaluation of the material, information was gathered from the literature about the performance of conventional aluminum alloys. A sample of material was obtained from Eagle Pitcher Ltd. to examine the material. The compositional specification and heat specific material properties of the sample that was supplied by the company are included in Table 2.2. Physical and mechanical properties of the material were studied to determine the impact of boron addition on these properties. Mechanical properties were measured by performing tensile tests at ambient and elevated temperatures. In addition, differential thermal analysis was conducted to verify the melting point and thermal stability of the alloy. This was to establish the structural and chemical stability during a design basis fire.

Table 2.2: General and Heat Specific* Compositional Information and Properties for 1100 Borated Aluminum Alloy [7, 8]

Elements	Heat # 34437 *	1100 Alloy (Wt. %)
Si	0.27	1.0 – Fe Max
Fe	0.43	1.0 – Si Max
Cu	0.12	0.05-0.20
Mn	0.0	0.05 Max.
Zn.	0.01	0.01 Max
Others	Not reported	0.05 each, 0.15 Max total
Boron	4.6	N/A
^{10}B enrichment	95 Min.	N/A
Property	**Heat # 34437 ***	**Typical 1100**
Thermal Conductivity	198.8 W-m/K	222 W-m/K
^{10}B Areal Density	60.4 mg/cm^2	N/A

* denotes values for the specific to the heat # 34437

Aqueous corrosion tests were performed to compare the pitting susceptibility and corrosion rate in relation to other aluminum alloys. A large body of data for conventional aluminum alloys exists of the atmospheric corrosion rates over long time frames. By comparing the borated alloy to conventional alloys in aqueous corrosion tests, long term atmospheric corrosion rates could be estimated. The corrosion rate could be used to estimate the amount of boron released from the plate over the design life of the facility.

3. Properties

3.1 Physical Properties

A differential thermal analysis was conducted on a portion of the samples of the 1100 alloy and the results are in Figure 3.1. The melting point of the alloy is clearly denoted by the endothermic peak on heating and exothermic peak on cooling. From this plot, it is evident that the endothermic transformation of melting starts at ~ 630 to 640 ºC, which represents the solidus of the alloy. The liquidus or the point at which the alloy is completely molten was measured to be between 650 and 660 ºC. The Metals Handbook [8] lists the melting range of alloy 1100 to be between 643 (solidus) and 657 ºC (liquidus). This experiment illustrates that the addition of boron and impurities related to processing do not significantly lower the melting point of the alloy.

The eutectic composition between Al and AlB_2 phases is reported to be 0.022 wt. % B at 659.7 ºC which is very close to the liquidus of the alloy [9]. This is consistent with boron primarily present in the form of binary AlB_2. Also, it can be noted that there is an absence of any specific peak prior to melting. This indicates that significant phases present in the alloy are stable up to the melting range. The temperature

regime discussed above is well above that expected for a design basis fire. In summary, the borated aluminum alloy 1100 will be thermally stable and unaltered well beyond any temperature excursions expected during its service life.

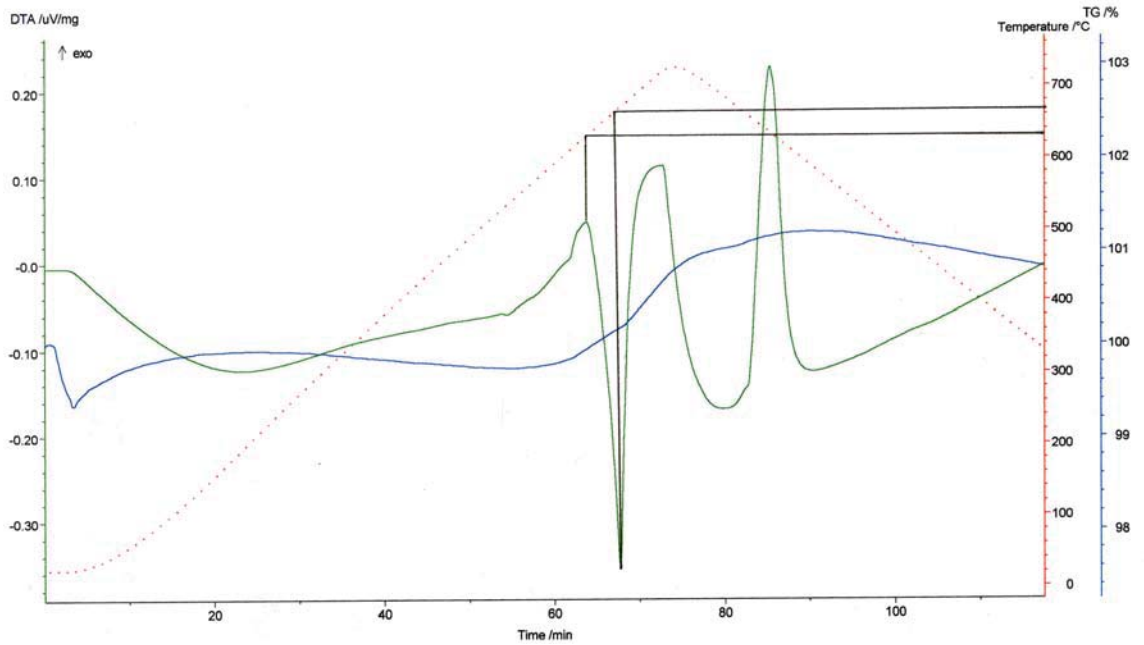

Figure 3.1: DTA plot of 1100 borated alloy with solidus and liquidus temperatures annotated

The microstructure of the borated aluminum alloy reinforces the conclusions drawn from the thermal analysis. In Figure 3.2, an optical micrograph shows the microstructure of the borated 1100 alloy. A bimodal distribution of borides is distributed throughout an aluminum matrix. Upon closer examination the larger borides appear to be agglomerates of several smaller borides. In Figure 3.3, a backscattered electron micrograph shows this microstructure at higher magnification. In this micrograph, impurity phases become evident, which contained aluminum, iron and silicon by energy dispersive spectroscopy (EDS). The presence of the phases is consistent with the microstructure of the 1100 alloy, which is noted to have the Al_3Fe phase present in wrought microstructures. Silicon is also a common impurity in alloy 1100.

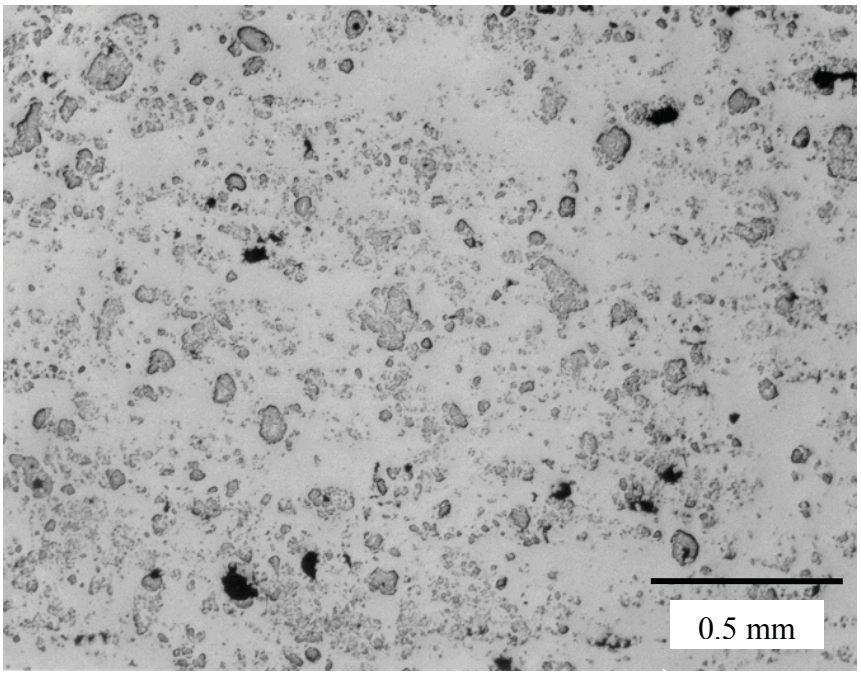

Figure 3.2: Optical micrograph of borated aluminum showing the distribution and scale of borides.

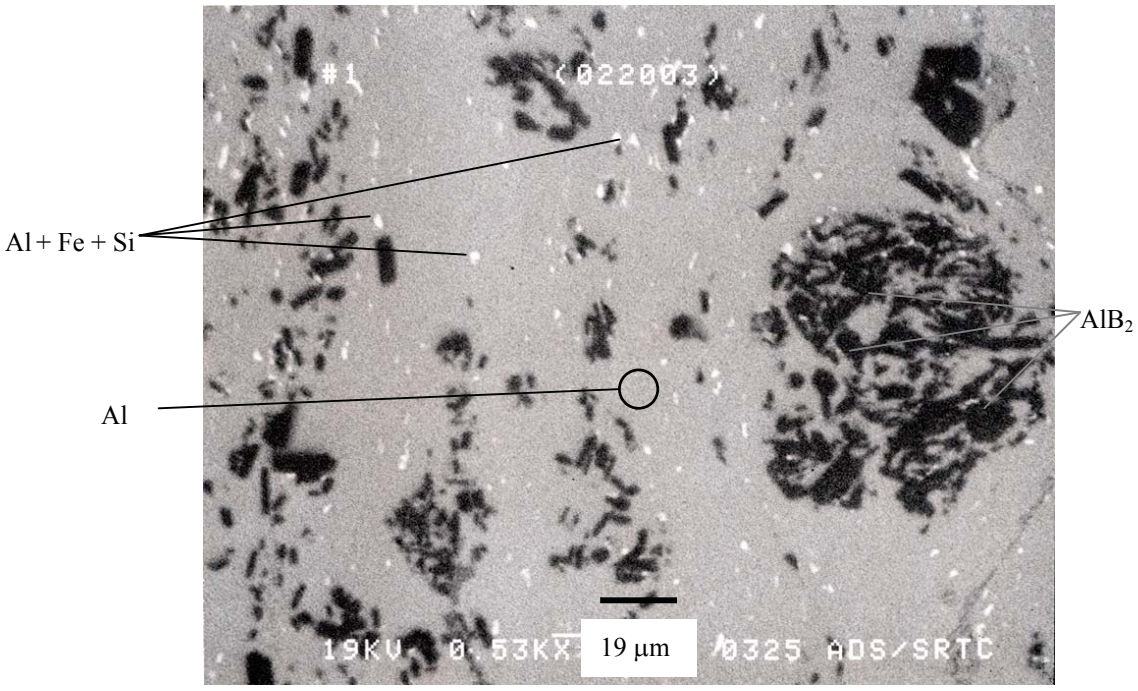

Figure 3.3: Backscattered electron micrograph showing the distribution of phases on a micron scale.

3.2 Mechanical Properties

The mechanical properties of the borated aluminum plate material at the temperatures of service and accident conditions are needed to verify structural stability. That is, any settling or embrittlement that leads to a redistribution of the borides may result in them no longer being effective neutron absorbers. Furthermore, the chemical analysis of the fracture surfaces of mechanical test specimens, in conjunction with physical characterization results described above, are used to show that the potential for redistribution of the boron is not significant.

Tensile tests at ambient and elevated temperatures were performed in adherence to the ASTM E8 specification [10] for tensile testing of metallic materials. Dog-bone type specimens were machined by electro-discharge machining (EDM) with a gage length of 1.0"long x 0.25" wide x 0.2" thick. The specimens were pulled at a strain rate of 8.3×10^{-4} sec^{-1}. The surface was not ground or polished prior to testing. The elevated temperature tests were performed on the same load frame with temperature being controlled with a convection furnace. The samples were soaked at temperature for 1 hr prior to testing to minimize temperature gradients.

Figure 3.4 shows the stress-strain curve for the tensile tests at room temperature, 250 and 558 ºF. The wide variability in tensile ductilities is due to the large concentration of hard borides, which cause stress concentrations around their interfacial regions with the aluminum matrix. The elongation for tensile specimens oriented with the tensile axis parallel to the rolling direction (i.e., longitudinal) is larger than that of the perpendicularly oriented specimen (i.e., transverse). The reason is apparent when examining the fracture surfaces. In Figure 3.5 a and b, scanning electron micrographs show images of the fracture surface of longitudinal and transverse specimens, respectively. A large number of particles line up with one another in distinct linear artifacts (see Figure 3.6). Such defects will propagate void growth easily and limit the deformation prior to failure.

In addition to aluminum borides many inclusions were observed on both fracture surfaces that contained elements other than aluminum, iron and silicon. Specifically, stringer compounds of containing K, Na, F, and Cl were observed on the fracture surface (see Figure 3.6). These elements were not observed on the metallographic sample but may only be visible on a fresh surface or along the boundary between the matrix and the boride due to the solubility of these elements in water.

The elevated temperature tensile tests show that the yield strength drops between 250 and 558 ºF and a drop in the strain hardening rate prior to 121 ºC (250 ºF). This means that a yield strength drop is not anticipated during the design basis fire and therefore the alloy should not undergo any significant structural change. The tensile curve at 292 ºC (558 ºF) exhibits a markedly lower yield point and actually exhibits a negative slope in the stress vs. strain curve at higher elongation. This behavior is consistent with materials that are beginning to undergo creep deformation. This temperature is actually at 60% of the alloy's melting point and as such is sufficient to overcome the activation energy required for deformation by creep.

These results were compared to typical properties for fully annealed 1100 aluminum (1100-O). The tabulated properties are included in Table 3.1. The properties of this heat of borated aluminum product meet or exceed the typical properties of the 1100-O alloy except in the elongation. This can be understood when consideration is given to the large quantities of borides present, which limit the ductility of this alloy. In spite of this, the properties are very close to 1100 without boron.

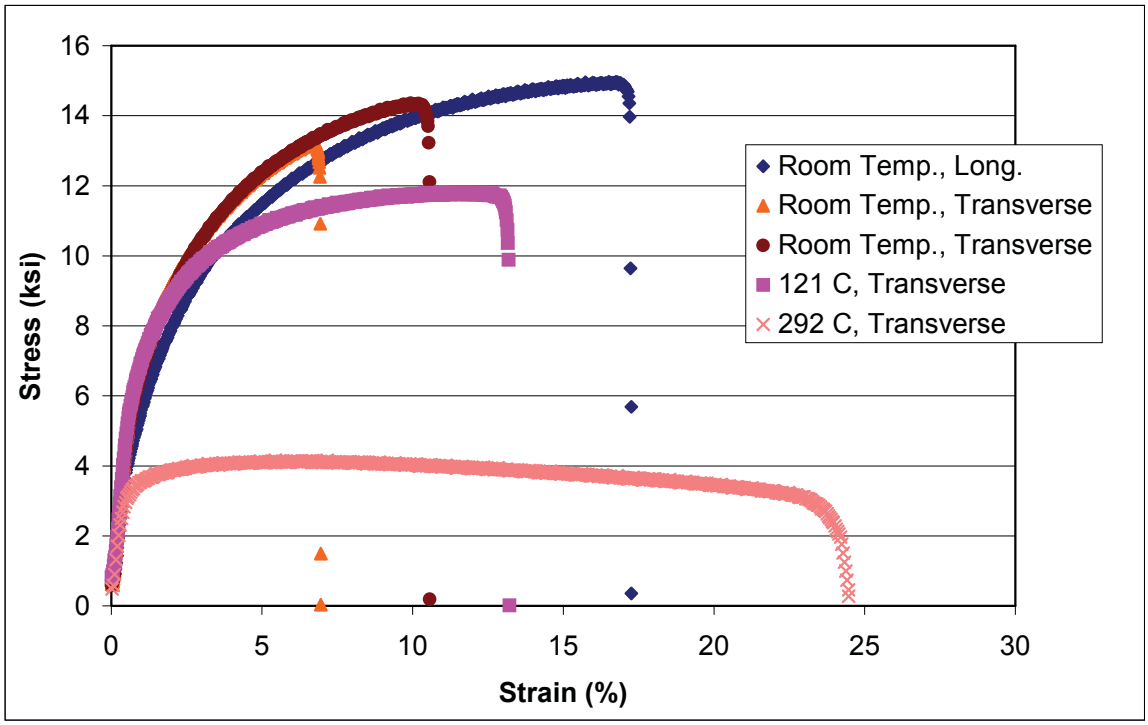

Figure 3.4: Engineering stress vs. strain curves of borated aluminum 1100 alloy at ambient and elevated temperatures

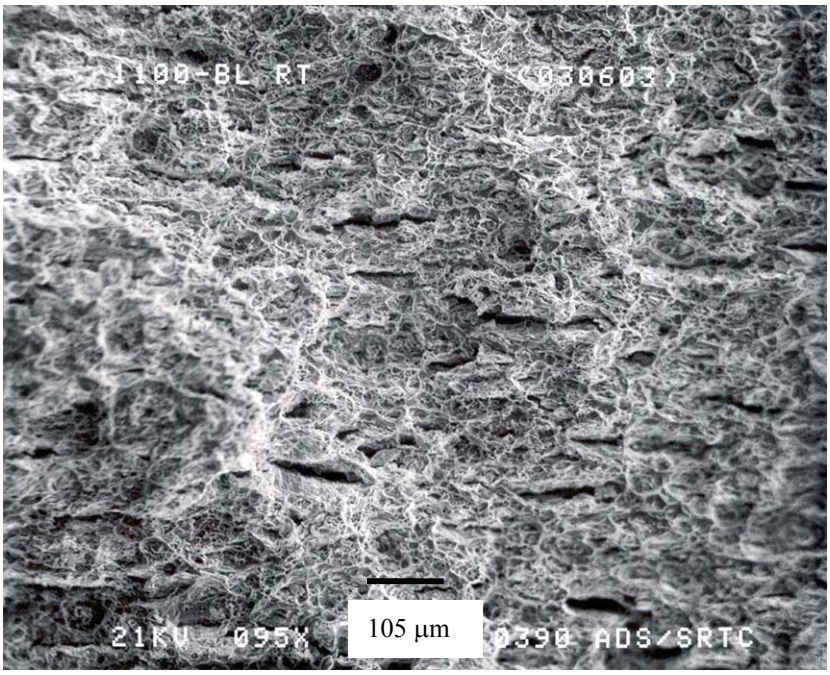

a)

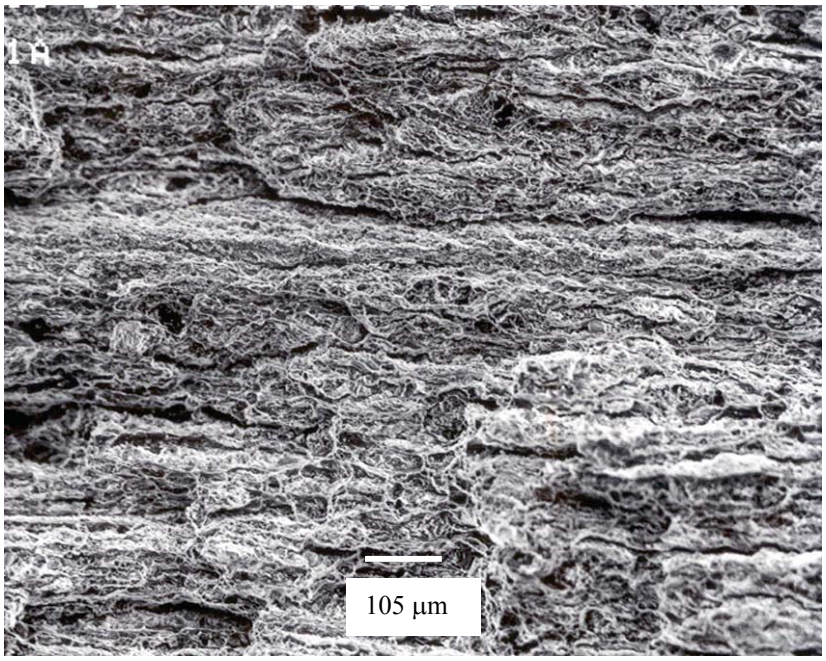

b)

Figure 3.5: Scanning electron micrographs comparing the fracture surfaces of tensile specimens oriented longitudinally a) and tranversely b) with respect to the rolling direction.

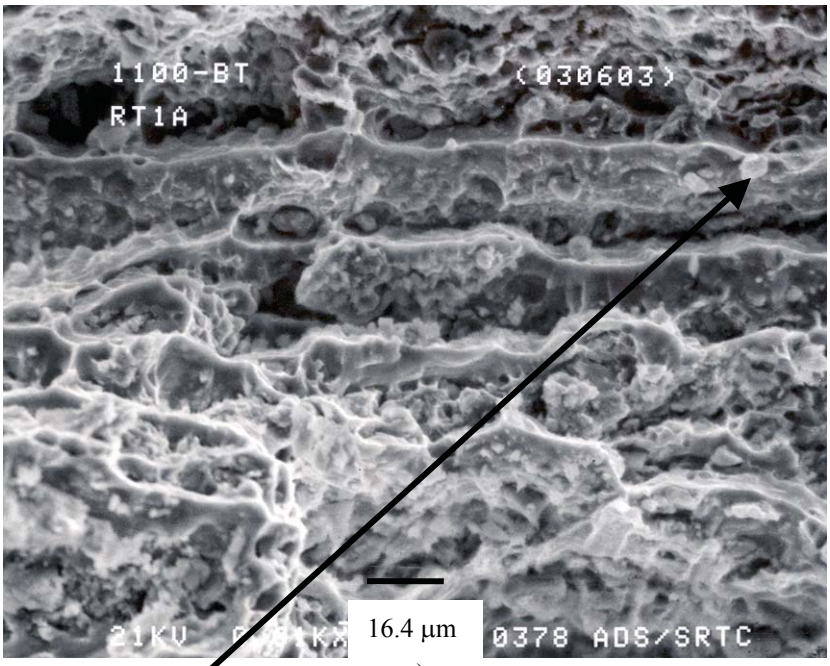

a)

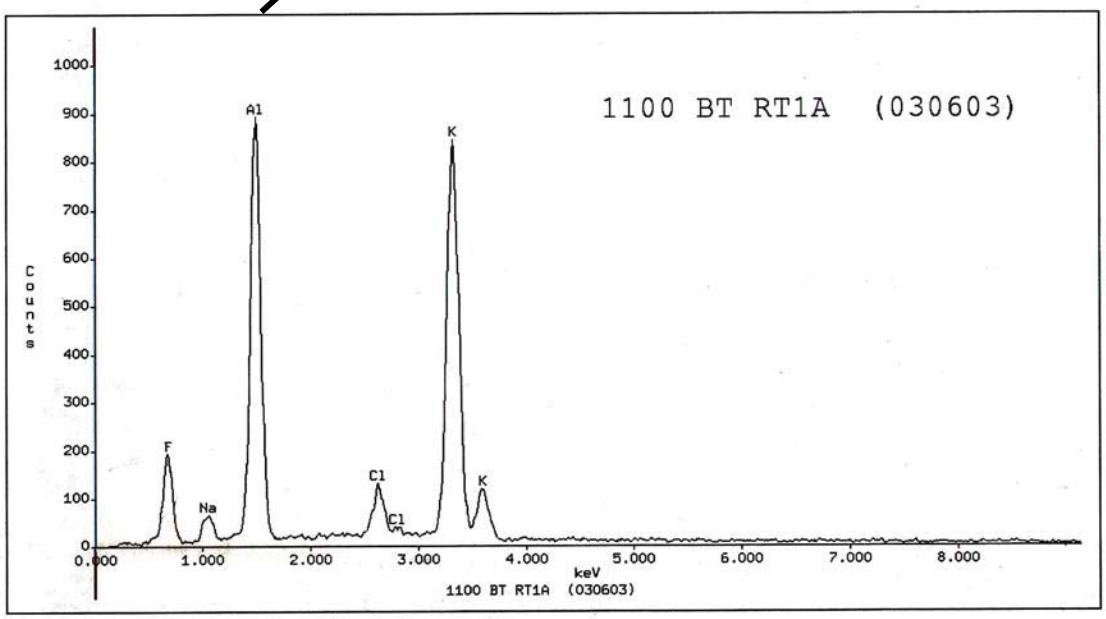

b)

Figure 3.6: Secondary electron micrograph of particles at the fracture surface a) and their complimentary EDS spectra in transversely oriented borated aluminum.

Table 3.1: Tensile properties from testing performed on 1100 borated aluminum with typical properties from alloy 1100 [8].

Specimen	Orientation	Temperature °C (°F)	Yield (ksi)	UTS (ksi)	Elongation (%)
1100BLRT	Longitudinal	25 (77)	4.9	14.9	17.1
1100BTRT	Transverse	25 (77)	7.1	13.2	6.7
1100BTRT1	Transverse	25 (77)	6.3	14.3	10.3
1100BT121	Transverse	121 (250)	6.3	11.8	12.6
1100BT292	Transverse	292(558)	3.1	4.1	23.1
1100-O [8]		24 (75)	5 (min 3.5)	13 (min 11)	40 (min 15)
		100 (212)	4.6	10	45
		149 (300)	4.2	8	55
		204 (400)	3.5	6	65
		260 (500)	2.6	4	75

3.3 Corrosion Properties

Atmospheric corrosion of aluminum is a complex process of chemical reactions that occur between the base metal and its environment over time. The presence of pollutants and water in the air increase the rate of reactions dramatically because they work together to break down the passive oxide layer on the surface of aluminum. Of the pollutants most common in the air, sulfur and chlorine containing compounds are the most deleterious substances [11]. These substances react with water to form anions (SO_4^{2-} and Cl^-) and in adsorbed surface water help break down the passive film that is normally stable on aluminum in air. Several years worth of atmospheric corrosion data exists for aluminum in numerous environments. Table 3.2 lists some of the data for atmospheric corrosion of aluminum. From data like these, numerous models have been proposed for the indoor and outdoor corrosion rate of aluminum in industrial, rural and urban environments. The majority of these models rely on three variables. Time of wetness (TOW) is the number of hours in the year that the relative humidity is above 80% and the temperature is above 0 ºC. The other variables are dependent on the deposition rates of SO_2/SO_4^{2-} and Cl^-.

The ISO 9223 [12] standard entitled, "Classification for the Corrosivity of Atmospheres" predicts degradation rates for aluminum and other metals as a function of these three variables. The standard divides all environments into five levels of corrosivity (denoted C1-C5). The corrosion rates predicted range from negligible to 0.073 - 0.145 mpy (5-10 g/m^2yr). Roberge et al. [13] reviewed this standard and gave guidance on how to categorize environments. Table 3.3 shows the predicted aluminum corrosion rates based on the ISO 9223 standard for indoor environments with (TOW < 10 hours/year) and without climate control (10 < TOW < 250 hours/year). The levels of chloride and sulfide must be high to produce corrosion rates of more than 2 g/m^2yr. This is equivalent to 0.029 mils/year.

Table 3.2: Measured Atmospheric Corrosion Rates of Various Aluminum Alloys for Different Environments [14]

Aluminum Alloy	Environment	Years of Exposure	Corrosion Rate (mpy)	Corrosion Rate (g/m^2yr)
1100-H14	average*	7	0.0136	0.9
1100-H14	Arid	20	0.003	0.2
1100-H14	Rural	20	0.003	0.2
1100-H14	Seacoast	20	0.011	0.8
1100-H14	Seacoast	20	0.023	1.6
1100-H14	Industrial	20	0.0295	2.0
1135-H14	average*	7	0.0126	0.9
1188-H14	average*	7	0.0098	0.7
1199-H14	average*	7	0.0081	0.6
6051-T4	Arid	20	0.0005	0.0
6051-T4	Rural	20	0.003	0.2
6051-T4	Seacoast	20	0.0135	0.9
6051-T4	Seacoast	20	0.0305	2.1
6051-T4	Industrial	20	0.036	2.5
6061-T4	average*	7	0.0149	1.0
6061-T6	average*	7	0.0166	1.1

*rates averaged between seacoast and industrial environments

Table 3.3: Predicted Short Term Corrosion Rates for Aluminum Alloys in Various Indoor Environments [12] (shading denotes TOW values for indoor environments w/climate adequate control)

Time of Wetness , TOW (hours/year)	Chloride Content (mg/m^2day)	Sulfur Dioxide Content (mg/m^2day)	Predicted Corrosion Rate	
			(mpy)	(g/m^2year)
<10	≤ 60	≤ 200	Negligible	negligible
<10	61-300	≤ 80	≤ 0.0087	≤ 0.6
<10	61-300	81-200	≤ 0.029	≤ 2.0
10-250	≤ 60	≤ 35	Negligible	negligible
10-250	≤ 60	36-80	≤ 0.0087	≤ 0.6
10-250	≤ 60	81-200	0.0087 - 0.073	0.6 – 5.0
10-250	61-300	≤ 35	0.0087 - 0.029	0.6 – 2.0
10-250	61-300	36-80	0.0087 - 0.073	0.6 – 5.0
10-250	61-300	81-200	0.029 - 0.073	2.0 – 5.0

To compare the borated aluminum alloy to conventional aluminum alloys, electrochemical and coupon immersion testing were performed with coupons of three different alloys. In these test the borated aluminum was studied along with conventional 1100 and 6061 aluminum alloys to provide a relative comparison of corrosion behavior. Several ASTM standards were used as guidelines during testing [15,16,17, 18, 19, 20, 21, 22]. Table 3.4 shows the measured corrosion rates in 5 ppm and 30 ppm Cl^- containing solutions determined from linear polarization at 30 ºC. The corrosion rates were similar for all three alloys. The results range from 0.1 to almost 1 mil per year.

The role of pitting in the atmospheric corrosion can be important in determining the overall rate of degradation and the boron loss. Cyclic polarization experiments are used to assess the susceptibility to pitting for a material in a particular solution. Previous studies by Chandler et al. [[23]] showed that 1100 alloys did not pit in a solution of 7.5 ppm Cl^- but did at 30 ppm, while 6061 exhibited pitting in both solutions. In order to compare the borated aluminum alloy with both 1100 and 6061 alloys, cyclic polarization test were also performed in the 5 and 30 ppm Cl^- solutions. In Figure 3.7 a and b, the cyclic polarization curves are shown for the 5 ppm and 30 ppm solutions, respectively. The curves display hysteresis in the current between the forward and reverse scans. The larger reverse-scan current is indicative of pitting susceptibility. When comparing the 1100 and 1100 +B alloys, it is evident that their curves resemble each other. Hence, it would appear that borated aluminum it not more susceptible to pitting than 1100. This further illustrates the similarities between the two alloys. However, the 6061 curves do show a marked hysteresis compared to the other curves. This work confirms observations made by Chandler et al. [23], where 6061 was observed to exhibit an increased pitting susceptibility in chloride solutions. The relative voltages of the minimum in current density would indicate that the 1100 + B alloy is the most active surface, followed by the 1100 alloy and then the 6061 alloy.

In addition to polarization studies, static immersion tests were conducted in the 5 and 30 ppm Cl- solution at 30 ºC. Figure 3.8 shows photographs of each alloy after 21 days in the 5 ppm solution. As is evident, very little difference was observed among the alloys. Optical micrographs show corrosion products forming with nodules protruding from the surface of each coupon. Further work may be conducted to determine if there are differences in pit density, but this initial evaluation does not note any significant difference in the corrosion behavior of the boron containing alloy. This enables the use of previous experimental data and models to predict the amount of boron loss over time as a result of environmental degradation.

Table 3.4: Aqueous Corrosion rate from linear polarization at 30 ºC

Sample	5 ppm Cl^- (mpy)	30 ppm Cl^- (mpy)
1100	0.5-0.9	0.9
6061	0.1	0.2
1100 + Boral	0.3	0.3

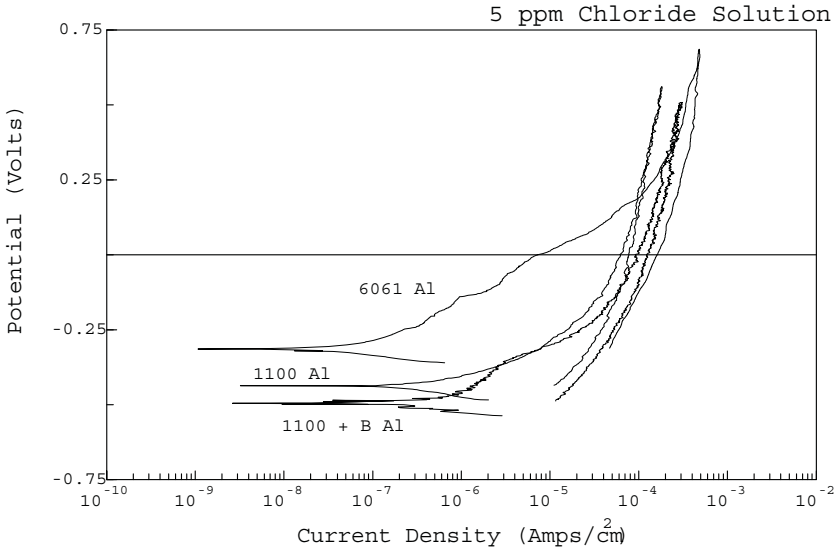

a)

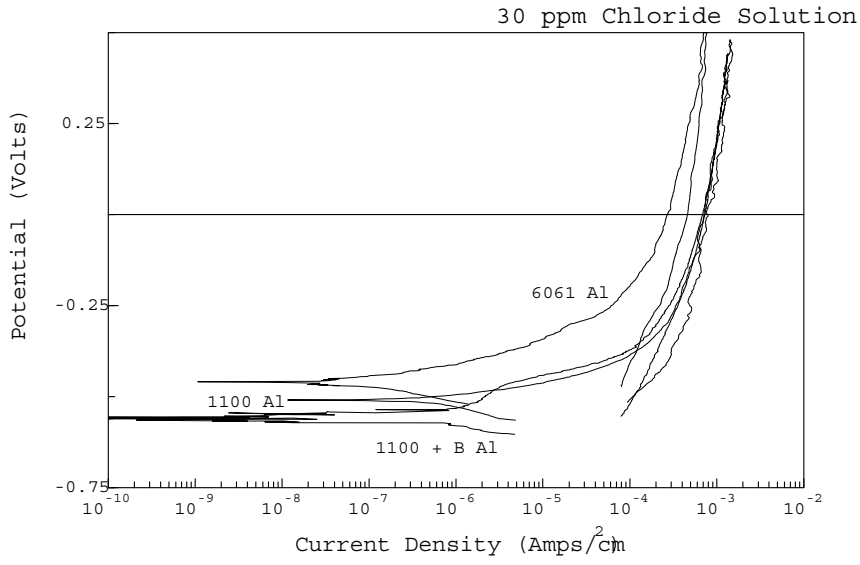

b)

Figure 3.7: Cyclic polarization curves for three aluminum alloys in 5 ppm Cl- a) and 30 ppm Cl- b) solutions.

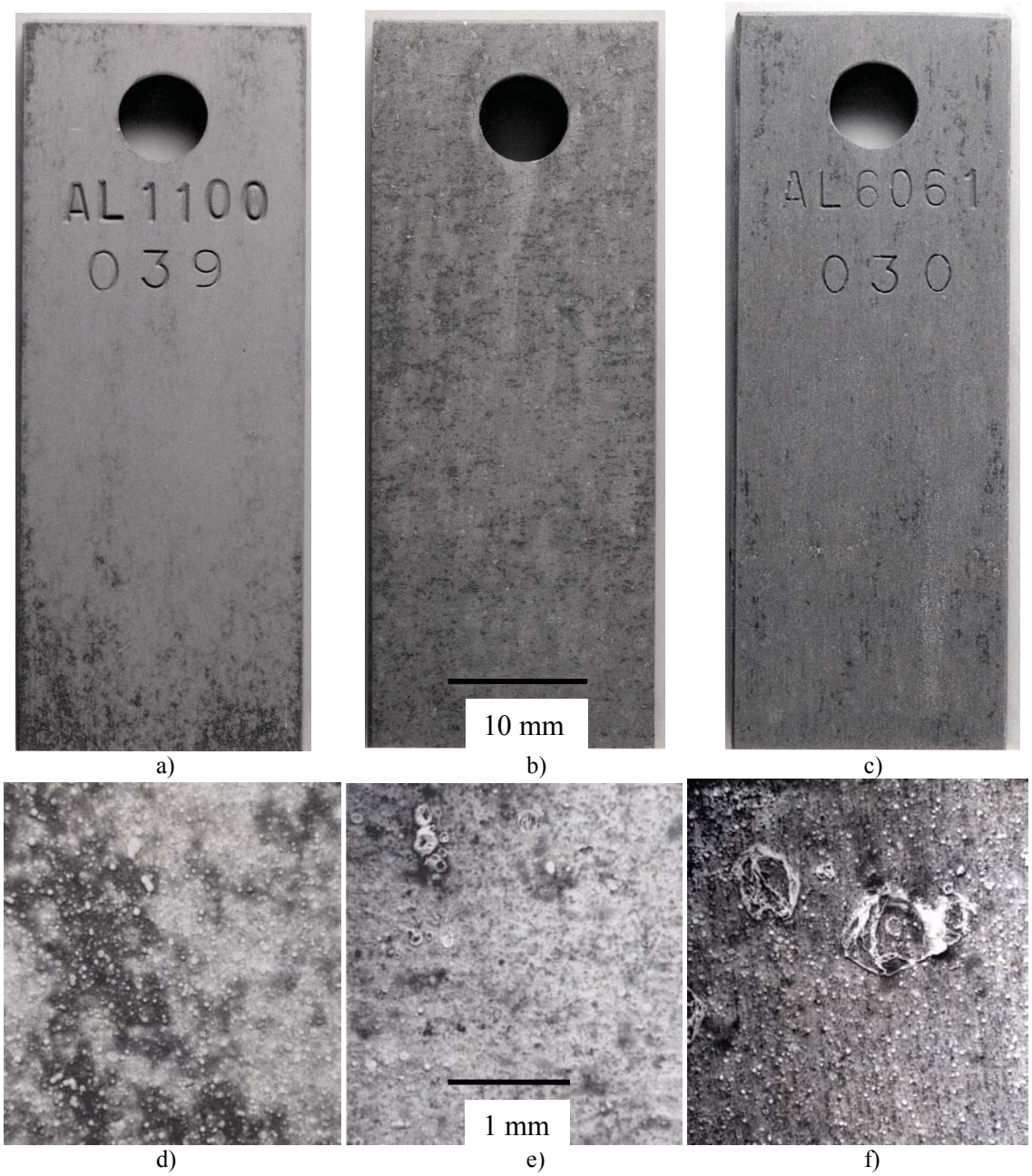

Figure 3.8 : Static corrosion immesion coupons after 21 days in 5 ppm Cl^- solution.

4. Boron Consumption

4.1 Environmental Degradation

Based on the corrosion evaluation discussed above, a corrosion rate can be selected to project the boron released from the alloy during the service life. Certain assumptions were necessary for this estimate. They are listed below.

- A bounding condition for the atmospheric corrosion rate is 0.029 mils/year (2 g/m^2yr) for the borated aluminum alloy.
- Corrosion occurs uniformly from both sides (i.e., 2X the surface area of corrosion from one side) of a semi-infinite sheet that is 7 mm in thickness (0.276") and contains 2.0 weight % boron (95% enriched) uniformly distributed in the aluminum matrix.
- The surface area and corrosion rate are constant over time
- The density of the alloy is 2.71 g/cm^3
- The time of corrosion is 20 years
- The boron leaves the system after release from the aluminum alloy.

The essential variables and calculated degradation rate are listed in Table 4.1. As is evident, less than ½ % of boron would be lost as a result of atmospheric corrosion.

Table 4.1: Essential Variables and Estimated Loss of Boron due to Atmospheric Corrosion during the 20 year Service Life.

Variable	Estimated Value
Volume/m^2 (m^3/m^2)	0.007
Mass of Sheet/m^2 (g/m^2)	18970
Mass of Boron/m^2 (g/m^2)	379.4 (360 g ^{10}B)
Loss of Material/m^2 ($g/y/m^2$)	4
Loss of Boron/m^2 ($g/y/m^2$)	0.08 (0.076 g ^{10}B)
Loss of Boron after 20 years (wt. %)	0.42

4.2 Boron Consumption by Nuclear Reactions

The potential reduction of boron content as a result of neutron sources produced by spontaneous fission and the alpha neutron reactions is estimated here. In this case these neutrons will deplete the B-10 absorbers distributed in the borated aluminum. Previously an almost identical approach was used to determine the boron consumption in K-area storage racks [24]. The only difference between the approaches is the material and geometric differences between the storage configurations. Detailed descriptions for the boron depletion calculations are provided below.

Source Term for Present System

The potential boron depletion in aluminum sheet is derived from neutron source computations. The absorption in B-10 is affected by whether the storage area is dry or flooded. The B-10 absorption cross section ($\sigma_a \approx$ 3,720 barns) is much larger for thermalized neutrons than for the fast neutrons ($\sigma_a \approx$ 5 barns at 0.1Mev neutron). Hence, when water or other neutron moderators are present interaction between boron and neutrons is much greater than when no water is present. Thus, the presence of water leads to an increase boron consumption.

In this situation, the present calculation took a conservative approach, which bounds the possibilities of having moderators present or absent. It was assumed that all neutrons available in the storage system were thermalized and therefore, contributed to the B-10 consumption. Main assumptions for the boron depletion computations were used as follows:

- The present model does not explicitly account for the spatial distributions of the fissile or fissionable isotopes and neutrons, assuming that all physical parameters are representative of the values averaged over the mass of fuel contained in the modeling domain.
- The present model calculations are based on a single-energy group assumption.
- All fissile materials are assumed to be 100% Pu-239 or a mixture of Pu-239 and Pu-240 so that no fission products are present. The depletion of fissile materials and their effect on boron depletion is negligible since a large number of fissile material nuclei exist in the storage system.
- The fissile material is a metallic based alloy minimizing the contribution of (α, n) reactions between α particles and oxygen in the canister.
- Boron nuclei are homogeneously distributed in the vicinity with enriched boron compositions (about 95 w/o B-10).
- All source neutrons generated in storage rack are completely absorbed into B-10 nuclide for an adequate conservatism neglecting neutron leakage and additional absorption in materials other than the B-10.
- Keff = Ksafe (0.95) was used to determine the number of neutron produced by spontaneous fission.

Based on these modeling approaches and assumptions, neutron source terms are established to estimate the boron depletion as function of fuel storage time in the present rack configurations.

Analysis of Neutron Source Terms

Neutron source terms are required to estimate the boron depletion with respect to fuel storage time in aluminum plates. Initial neutron source rate (S^n) in fissile plutonium storage rack comes from neutron source terms arising from, spontaneous fission (SF), (α, n) reactions, and photoneutrons due to radioactive decay (γ, n).

$$S^n = S_{SF}{}^n + S_{(\alpha,n)}{}^n + S_{(\gamma,n)}{}^n \quad (1)$$

Detailed discussions on these three main contributions of neutron source are provided previously [24]. A brief discussion of the primary source (i.e., spontaneous fission) is provided below. The contributions of neutrons derived by (α, n) reactions or photoneutrons are assumed to be negligible.

Source Contribution from Spontaneous Fission

The rate of neutron emission from spontaneous fission events for a fissionable nuclide i, $S_{SF_i}{}^n$, is calculated from the atom density of the spontaneously fissioning isotope, N_i, its decay constant, λ_i, the branching fraction for spontaneous fission, ε_i, and the average number of neutrons emitted per fission, ν_i. That is

$$S_{SF_i}{}^n = N_i \lambda_i \varepsilon_i \upsilon_i \quad (2)$$

where i represents fissioning isotope.

As discussed earlier, the present work assumes that there are no uranium isotopes such as U-235 and U-238 or actinide products such as Am-241 and Cm-244 nuclides produced as result of high fuel burnup. In addition, the amount of Pu-238 is also considered to be negligible. In this situation neutron source contributions made from the spontaneous fission of Pu-239 and Pu-240 nuclides present in concentrated quantities are dominant. Thus total neutron source produced from the spontaneous fission $S_{SF}{}^{n}$ can be obtained by summing up the contributions from all fissionable nuclides available in the storage racks.

$$S_{SF}{}^{n} = \sum_{i} N_i \lambda_i \varepsilon_i \upsilon_i \qquad (3)$$

Table 4.3 shows physical values for the modeling parameters used in eq. (2). As is evident the fraction of spontaneous fission (ε_i) for Pu-240 is 4 orders of magnitude greater than that of Pu-239. This makes the neutron source term extremely sensitive to the Pu-240 content. Pu-238 and Cm-244 would also have significant effects on the source term if present in significant quantities.

Table 4.2 Nuclear Decay Constant and Branching Fraction of Spontaneous Fission for Heavy Radionuclides [25]

Isotopes	Relative amount in current storage system	Decay constant (λ_i)	Fraction of spontaneous fission (ε_i)	Number of neutrons emitted per fission event (ν_i)
U-235	None	9.72×10^{-10} yr^{-1}	4.20×10^{-10}	2.3
U-238	None	1.54×10^{-10} yr^{-1}	5.40×10^{-7}	2.3
Pu-238	None	7.67×10^{-3} yr^{-1}	1.84×10^{-9}	2.3
Pu-239	80-100%	2.84×10^{-5} yr^{-1}	4.40×10^{-12}	2.2
Pu-240	0-20%	1.1×10^{-4} yr^{-1}	4.95×10^{-8}	2.2
Am-241	None	1.49×10^{-3} yr^{-1}	3.77×10^{-12}	2.4
Cm-244	None	3.78×10^{-2} yr^{-1}	1.35×10^{-6}	2.8

Source Contribution from (α, n) and Photoneutron Reactions

The interaction of alpha particles or gamma rays on nuclei of certain light elements produces neutrons. In some cases, significant contributions to the source term result from these interactions. As discussed earlier, most neutrons released are from spontaneous fission, but the (α, n) and (γ, n) reactions provide a smaller contribution to the neutron source available for the boron depletion.

The interaction of alpha particles with nuclei of lithium, beryllium, boron, and fluorine produces neutrons. Neutrons from this source may be important to shielding and safety during storage. This (α, n) reaction occurs when alpha particles from the actinide isotopes interact with certain elements present in actinide compounds. Thus, α-producing actinides (e.g., Pu-239, Pu-240), in the presence boron or oxygen, may lead to the generation of neutrons by interactions of the alpha particles with these light elements. Canisters filled with metal have limited amounts of oxygen or light elements in them. The presence of boron atoms in the vicinity of the canister has little effect on (α, n) reaction, because the alpha particles can not escape the plutonium or the canister to reach and interact with the boron containing material. The only significant

source of neutrons from (α, n) reactions are as a result of the presence of plutonium oxide within the canister. However, the contribution to the neutron source term is not significant compared to spontaneous fission when Pu-240 or Pu-238 are present in sufficient quantity. Hence, a source contribution from the (α, n) reaction is negligible and can be ignored for this approximation [26].

$$S_{(\alpha,n)}{}^{n} \approx 0.0 \tag{4}$$

It is possible to produce neutrons by the interaction of gamma rays on target nuclei. Certain nuclei have sufficiently low thresholds in gamma ray energy for this process to enable the construction of photoneutron sources. The few nuclei whose neutron binding energies are low enough to create a possible problem in storage area include D-2, Be-9, C-13, Li-6. The threshold photon energies for these isotopes are 2.23, 1.67, 4.9, and 5.3 MeV, respectively. In most cases, γ-ray emitters are short-life radionuclides and their target nuclei are light atoms such as beryllium, oxygen, or nitrogen. The present storage systems do not contain sufficient quantities of these materials to consider the (γ, n) reaction as a significant contribution to the source term. Thus, the contribution from photoneutron reactions is negligible.

$$S_{(\gamma,n)}{}^{n} \approx 0.0 \tag{5}$$

When eqs. (3) to (5) are applied to eq. (1), the final equation for neutron source rate of the present storage configurations becomes

$$S^{n} = \sum_{i} N_i \lambda_i \varepsilon_i \upsilon_i \tag{6}$$

Source Multiplication

When a radioactive material in a storage area includes fissile or fissionable isotopes, neutrons emitted from spontaneous fission will cause additional fissions to occur. When the fissile or fissionable isotopes are included in the material of a subcritical storage system, this subcritical multiplication should be considered to compute source neutrons. The effective multiplication factor k_{eff} applicable to the source term can be obtained from a criticality analysis for the storage configurations, which has been performed in the previous section.

Suppose the neutron source rate S^n, of which a fraction L escapes from the storage rack and a fraction k_{eff} appears as new neutrons, $S^n(1-L)k_{eff}$ are existing in the rack, while $S^n(1-L)(k_{eff})^2$ reproduce another generation. Therefore, the total number of neutrons per time S as the result of all such cycles is

$$S_{total} = S^n(1-L)\left(1 + k_{eff} + k_{eff}{}^2 + k_{eff}{}^3 + \cdots\cdots\right) \tag{7}$$

For a subcritical system, $k_{eff} < 1$, total neutron source rate S_{total} can be determined by use of the geometric progression series. That is

$$S_{total} = \frac{S^n(1-L)}{1-k_{eff}} \tag{8}$$

In this case no leakage ($L = 0$) through the storage system boundary is assumed for conservative estimation. Now conservative estimation of total neutron source from the present storage rack, S_{total}, can be made in terms of the current storage conditions and material properties. That is

$$S_{total} = \frac{\sum_{i} N_i \lambda_i \varepsilon_i \upsilon_i}{(1-k_{eff})} \tag{9}$$

In Figure 2.1, a picture of a racks used in the storage facility is shown. The borated aluminum is intended to be hung on the wall in the storage area behind each rack. The allowable area available for borated

aluminum is then wall area the rack occupies. The design of the rack has canisters positioned on an 8" wide x 18" high x 12" deep pitch. So the area allowed for borated aluminum some multiple of that number. The assumption of boron concentrations was 0.0359 g/cm2, which is the number for a 2% boron alloy of 7mm (0.276") thickness. The important material inventories in the 235-F storage facility are summarized in Table 4.3.

Table 4.3 Summary of Materials Used in Boron Depletion Model

Racks Positions	# slots in each rack	Pu Content (kg)	Wall area behind rack (m^2)	Amount of Boron behind each rack (g)
74 x 5 x 2	740	3256.0	32.46	11654.7
30 x 7 x 2	420	1848.0	18.43	6614.9
10 x 5 x 2	100	440.0	4.39	1575.0
27 x 5 x 2	270	1188.0	11.85	4252.4
27 x 5 x 2	270	1188.0	11.85	4252.4
17 x 5 x 2	170	748.0	7.46	2677.4
Total	**1970**	**8668.0**	**86.43**	**31026.8**

Since the K_{safe} = 0.95 and the calculated value of K_{eff} is within 3% of that value, a value of 0.95 was used to determine the number of neutron produced by spontaneous fission for all cases. This is conservative for all cases. However, the answer is extremely conservative for the cases with high concentration of Pu-240 (shaded in the table) which would certainly decrease the K_{eff} for the storage configuration.

The results of the analysis show that the B-10 depletes by a negligible amount for the assumptions shown in Table 4.10. A maximum fractional depletion of B-10 nuclei was determined to be only 1.1×10^{-8} of the B-10 loading over the next 20 years. The reference time denotes the "start" time used for calculational purposes. The results show that the uncertainties associated with various modeling assumptions can alter the results of the B-10 depletion, but the total value is still negligibly small, and will have little impact on rate of boron depletion during the proposed service life. Hence, the boron loss as a result of atmospheric corrosion can be used as the total boron depletion, since it is limiting.

Table 4.4: Results Summary for Boron Depletion by n-Absorption

Fully loaded 235-F storage configuration (Keff = 0.95)	Total Neutron Source available in 235-F (no. of neutrons per sec)	Fraction of B-10 depletion for storage time to B-10 contents at reference time	
		5 years of storage from reference time	20 years of storage from reference time
100% Pu-239	3.8×10^{6}	3.2×10^{-13}	1.3×10^{-12}
96% Pu-239 4% Pu-240	6.7×10^{9}	5.6×10^{-10}	2.2×10^{-9}
93% Pu-239 7% Pu-240	1.2×10^{10}	9.6×10^{-10}	3.8×10^{-9}
80% Pu-239 20% Pu-240	3.3×10^{10}	2.7×10^{-9}	1.1×10^{-8}

5. Conclusions

The results from this work can be used as inputs into the project design and implementation of aluminum based neutron absorbing materials in 235-F for criticality control.

- The physical, mechanical, and corrosion properties of conventional 1100-O aluminum alloy over the entire temperature range of service and accident conditions can be conservatively applied to borated aluminum alloy 1100. That is, the handbook values of properties are essentially the same, except that the ductility of the borated alloy is slightly less.
- Based on maximum rates (R=0.029 mils/year) of corrosion aluminum in environments similar to 235-F, less than ½ % of boron is predicted to be lost through corrosion of a plate structure 7 mm thick over the 20 year service life.
- Based on the approximate neutron source term for the present storage configuration a maximum fractional boron consumption of 1.1×10^{-8} was determined to occur over the 20 year service life.

No additional surveillances are needed to verify these conclusions. However, if a design-basis fire or other off-normal event occurs during the storage period, it is recommended to verify that the environmental conditions of the event have been covered by those assumed in this report for demonstration that a borated aluminum alloy would remain effective as a criticality control material for the planned use to line the walls of the 235-F vault.

6. References

1 Davoud Eghbali, 2/2003, private communication

2 Janice Hearn, 2/2003, private communication

3 National Atmospheric Deposition Program, 2001 Annual Summary, Champaign, IL, 2001

4 The Bureau of Air Quality, 1999 Annual Report, South Carolina Bureau of Air Quality, Aiken, SC 2001.

5 The Bureau of Air Quality, 2002 Annual Summary, South Carolina Bureau of Air Quality, Aiken, SC, 2002.

6 J. K. Norkus, S-CLC-K-00187 Rev. 0, Thermal Analysis of KAMS Fires (U), p. 165

7 Jim Hall, Eagle-Pitcher Technologies, 2/2003, private communication

8 Metals Handbook, Ninth Edition, Volume 2, pg. 65, American Society for Materials, Materials Park, OH, 44073, 1979

9 T. B. Massalski, Handbook of Binary Phase Diagrams, American Society for Materials, Materials Park, OH, 44073, 1990

10 American Society for Testing and Materials, Designation E8, ASTM International, West Conshohoken, PA.

11 **Atmospheric Corrosion**, C. Leygraf and T.E. Gradedel, Electrochemical Society Series, Wiley Interscience Publ., New York, 2000

12 ISO 9223, "Corrosion of metals and alloys - Classification of corrosivity of atmospheres."

13 P. R. Roberge, R. D. Klassen and P. W. Haberecht, “Atmospheric Corrosivity Modeling- a review” Materials and Design, Volume 23 (2002) 321-330.

14 Metals Handbook, Ninth Edition, Volume 2, pg. 223, American Society for Materials, Materials Park, OH, 44073, 1979

15 American Society for Testing and Materials, Designation G1-90, ASTM International, West Conshohoken, PA.

16 American Society for Testing and Materials, Designation G3-89, ASTM International, West Conshohoken, PA.

17 American Society for Testing and Materials, Designation G31-72, ASTM International, West Conshohoken, PA.

18 American Society for Testing and Materials, Designation G46-76, ASTM International, West Conshohoken, PA.

19 American Society for Testing and Materials, Designation G46-76, ASTM International, West Conshohoken, PA.

20 American Society for Testing and Materials, Designation G59-97, ASTM International, West Conshohoken, PA.

21 American Society for Testing and Materials, Designation G61-86, ASTM International, West Conshohoken, PA.

22 American Society for Testing and Materials, Designation G102-89, ASTM International, West Conshohoken, PA.

23 G.T. Chandler, R.L. Sindelar and P.S. Lam, Evaluation of Water Chemistry on the Pitting Susceptibility of Aluminum, Corrosion 97, NACE Corrosion paper # 104, Houston, TX, (1997)

24 A. J. Duncan, S. Y. Lee and A.W. Serkiz, K-Area Storage Racks – Boron Contents and Criticality Surveillance Evaluation, WSRC-TR-2002-00442, October, 2002.

25 G. R. Caskey, Jr., Potential Radiation Damage-Storage Tanks for Liquid Radioactive Waste (U), WSRC-TR-92-350, August (1992)

[26] N. Ensslin, Passive Nondestructive Assay of Nuclear Material, NUREG CR-5550, US NRC, Washington D.C., 1991 pp. 339 & 345.